Rock and Soil Mechanics

Volume 42 | Issue 9 Article 8

12-15-2021

Analysis of stress-structural collapse mechanism of columnar jointed basalt under high stress

Jian-cong ZHANG
University of Chinese Academy of Sciences, Beijing 100049, China

Quan JIANG
University of Chinese Academy of Sciences, Beijing 100049, China, qjiang@whrsm.ac.cn

Xian-jie HAO
University of Chinese Academy of Sciences, Beijing 100049, China

Guang-liang FENG
University of Chinese Academy of Sciences, Beijing 100049, China

See next page for additional authors

Custom Citation

ZHANG Jian-cong, JIANG Quan, HAO Xian-jie, FENG Guang-liang, LI Shao-jun, WANG Zhi-lin, FAN Qi-xiang, . Analysis of stress-structural collapse mechanism of columnar jointed basalt under high stress[J]. Rock and Soil Mechanics, 2021, 42(9): 2556-2568.

Analysis of stress-structural collapse mechanism of columnar jointed basalt under high stress

Authors

Jian-cong ZHANG, Quan JIANG, Xian-jie HAO, Guang-liang FENG, Shao-jun LI, Zhi-lin WANG, and Qi-xiang FAN

Rock and Soil Mechanics 2021 42(9): 2556−2568 ISSN 1000−7598
https: //doi.org/10.16285/j.rsm.2021.5194 rocksoilmech.researchcommons.org/journal

Analysis of stress-structural collapse mechanism of columnar jointed basalt under high stress

ZHANG Jian-cong[1, 2], JIANG Quan[1, 2], HAO Xian-jie[1, 2], FENG Guang-liang[1, 2], LI Shao-jun[1, 2], WANG Zhi-lin[3], FAN Qi-xiang[3, 4]

1. State Key Laboratory of Geomechanics and Geotechnical Engineering, Institute of Rock and Soil Mechanics, Chinese Academy of Sciences, Wuhan, Hubei 430071, China

2. University of Chinese Academy of Sciences, Beijing 100049, China

3. China Three Gorges Construction Management Co., Ltd., Chengdu, Sichuan 610041, China

4. China Huaneng Group Co., Ltd., Beijing 100031, China

Abstract: Columnar jointed rock mass with unique joint network structure is a special type of jointed rock mass, which is a binary structure composed of high strength 'basalt block' and specific 'dominant joint'. Relaxation, opening and slippage of columnar jointed surfaces and disintegration of columns occur easily during excavation under high ground stress, which eventually lead to disastrous collapses in columnar jointed rock mass. The construction safety of underground engineering under high stress is severed restricted by it. By combining acoustic wave, borehole camera and other integrated in-situ testing technology and numerical simulation, the mechanism of stress-structural collapse in columnar jointed rock mass under high stress is studied based on multiple columnar jointed rock mass collapses at left bank tailwater connection pipe of Baihetan hydropower station. The proposed controlling measures of excavation and support are also provided. The key of columnar joined rock mass collapse is the redistribution of stress in surrounding rock mass after the excavation and the strong unloading relaxation of columnar joined basalt, which causes the opening of its internal joint surfaces and structural deterioration, result in the disintegration of basalt columns. Thus, the chain catastrophic process of continuous unloading relaxation and progressive collapse of columnar jointed rock mass is induced. The research can provide reference for the prediction and control of deformation and failure of jointed rock masses in underground engineering under high geo-stress.

Keywords: high-stress; columnar jointed rock mass; stress-structural collapse; in-situ test; numerical analysis

1 Introduction

Due to the complex diagenesis and long-term tectonic process, engineering rock masses that exist in certain geological and stress environment contain a large number of structural surfaces (e.g., bedding, joints, and fissures) of varying sizes[1]. Therefore, most engineering excavation objects are continuous−discontinuous fractured rock masses composed of structural planes (groups of joints/fracture planes) and structural bodies (rock matrix). Sun[2] defined the deformation and failure of engineering rock masses as the phenomenon of rock mass structure reorganization and structural coupling loss. Wang[3] emphasized that the structural properties of fractured rock masses are the basis for its physical and mechanical properties. The rock mass structure is the basis for analyzing the deformation and failure of fractured rock masses. In recent years, with the construction of many large-scale underground engineering projects, such as Dagangshan Hydropower Station[4], Jinping II Hydropower Station[5], and Shuangjiangkou Hydraulic Cavern[6], it is found that the excavation unloading of underground engineering under high in-situ stress inevitably leads to the relaxation, opening and slippage of original structural planes of the jointed rock mass, as well as the fracture and structural disintegration of the rock mass, which in turn leads to the instability of engineering rock mass.

Extensive fruitful research has been carried out on the failure, relaxation and stability of engineering rock masses with joints/structural planes. For example, Martin et al.[7] divided the failure modes of the surrounding rock into structural controlled, stress-structure controlled type, and stress controlled type, based on the dual indicators of rock mass structure and in-situ stress/rock strength ratio. Xiang et al.[8] summarized 18 typical wall rock failure modes from three levels: control factors, mechanical mechanisms, and occurrence conditions. According to a number of typical failure cases of hydropower stations, Dong et al.[9] summarized three types of failure modes of surrounding rock based on control factors: stress controlled type, structural plane controlled gravity-driven type, and combined structure plane and stress controlled type. Tang et al.[10] pointed out that the representative elementary volume (REV) of rock mass has multi-scale effects and

Received: 27 January 2020 Revised: 23 April 2021
This work was supported by the National Natural Science Foundation of China(U1965205, 5177925) and the International Partnership Program of Chinese Academy of Sciences(115242KYSB20160017).
First author: ZHANG Jian-cong, born in 1991, PhD, research interests: columnar joint rock mass mechanical properties and underground cavern stability. E-mail: zhangjiancong15@whrsm.ac.cn
Corresponding author: JIANG Quan, born in 1978, PhD, Professor, research interests: numerical simulation of underground engineering, large cavern stability, safety and disaster prevention. E-mail: qjiang@whrsm.ac.cn

uncertainties. The relationship between the REV and the geometrical elements of the structural plane is as follows: a smaller REV corresponds to a larger trace length, a smaller distance, and a larger variance of direction angle. Qin et al.[11] proposed a simulation method for predicting the macro-elastic parameters of REV in jointed rock masses. Zhang et al.[12] proposed a size-effect reduction method and joint reduction method for the strength parameters of jointed rock masses. Zhang et al.[13] considered the randomness of the geometric and mechanical parameters of structural planes and proposed a method to determine the REV scale of rock mass using the fracture network. Singh et al.[14] studied the strength and deformation characteristics of structural rock masses with different joint occurrences and spacing conditions. Ivars et al.[15] proposed a synthetic rock mass model (SRM), which simultaneously considers the strength of rock matrix and the occurrence and strength of structural plane, so as to obtain a direct expression of the engineering rock masses. Li et al.[16] studied the effect of structural planes during the unloading process of structural rock masses in the high slope at Three Gorges Ship Lock. Shen et al.[17] studied the unloading failure process of the granite at Three Gorges Permanent Ship Lock and found that the rock masses unloading of the second lock chamber and third lock chamber is mainly caused by the off-surface unloading rebound and slab cracking of the structural surface parallel to the excavation surface. Existing studies have shown that joints have a significant effect on the deformation and failure of engineering rock masses, and the deformation and failure of jointed rock masses under high-stress unloading is a complex mechanical process between joints and rock masses under repeated stress adjustment. Therefore, further in-depth field observation and back analysis of the failure of jointed rock masses under high stresses are of great significance for enriching and developing the stability analysis theory and engineering control technology of jointed rock masses in deep underground engineering.

As a type of rock mass with special joint network structures, columnar jointed rock masses have been widely exposed in many projects (i.e., Tongjiezi, Xiluodu)[18], especially in the dam foundation, diversion tunnel, and underground powerhouse of Baihetan Hydropower Station, providing new site conditions for an in-depth understanding of the unloading mechanical properties of columnar jointed rock masses. In recent years, Fan et al.[19−20] and Shi et al.[21] have conducted field investigations and in-situ tests on the deformation and relaxation characteristics of columnar joints under excavation and unloading. Jiang et al.[22−23], Duan et al.[24] and Pei et al.[25] have conducted long-term monitoring on the unloading and relaxation characteristics of columnar joint basalt on the left bank of Baihetan dam and the columnar joint of the diversion tunnel, revealing its transverse isotropic mechanical properties and time-dependent relaxation characteristics of excavation unloading; Xiao et al.[26−27] and Ji et al.[28] performed experimental researches with anisotropic columnar jointed rock mass models under different column inclination angles by using similar materials such as gypsum and cement. Xu and his coworkers[29−33] established a geometric generalization model based on the basic characteristics of columnar jointed rock masses and estimated the equivalent deformation and strength parameters of columnar joints at different scales as well as macroscopic mechanical properties of columnar joints using the discrete element software (3DEC). These works are helpful for a comprehensive understanding of the columnar jointed mechanical properties. However, due to the unique geometry of the columnar jointed rock, engineering disasters such as stress-structural collapse often occur under the combined effect of complex rock geology of Baihetan Hydropower Station (such as dislocation zones, steeply inclined joint surfaces, faults and other unfavourable structural surfaces) and high stress field. Therefore, it is necessary to further reveal the mechanism of columnar jointed rock mass stress-structural collapse through in-situ observation and numerical back analysis, to ensure the safe excavation of underground caverns under high stress.

To this end, this paper aims at the columnar joint area collapse of the tailwater connection pipe on the left bank of Baihetan Hydropower Station. Field investigation, borehole camera testing of rock mass structure, and ultrasonic testing of the relaxation depth and degree of the surrounding rock are carried out to reveal the disaster characteristics and formation mechanism of the stress-structural collapse in columnar jointed rock masses. The three-dimensional numerical simulation method is then used to back-analyze the complex mechanical response and failure cause of surrounding rock in the columnar jointed rock mass collapse area. It is proposed that a chain catastrophe process that the opening and structural deterioration of the internal joint surface of the columnar jointed basalt leads to the fracture and disintegration of the basalt column, thereby inducing the continuous unloading and relaxation of the rock mass, as well as the gradual collapse. Meanwhile, targeted excavation and support control measures are proposed, which can provide a reference for deformation and failure analysis and landslide prevention of the same type of jointed rock masses under deep/high stresses.

2 Engineering background

2.1 Brief introduction to the underground tunnels

Baihetan Hydropower Station is located at the junction of Ningnan County (Sichuan Province) and Qiaojia County (Yunnan Province) on the lower reaches of the Jinsha

River. The underground powerhouses on the left and right banks are each equipped with eight 1 000 MW vertical hydroelectric generators with a total installed capacity of 16 000 MW, which is the second-largest hydropower station in China after the Three Gorges Hydropower Station[34]. The left and right banks of the diversion and power generation system of hydropower stations are symmetrically arranged. The underground cavern groups includes main powerhouse, main transformer chamber, busbar chamber, tailwater connection pipe, tailwater connection pipe repair gate chamber, and tailwater surge tank.(see Fig.1(a)).

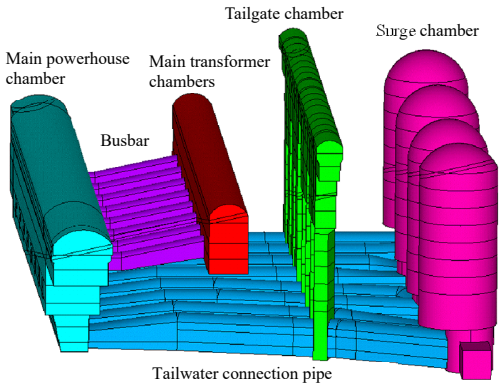

(a) 3D model of the main chambers at the left bank

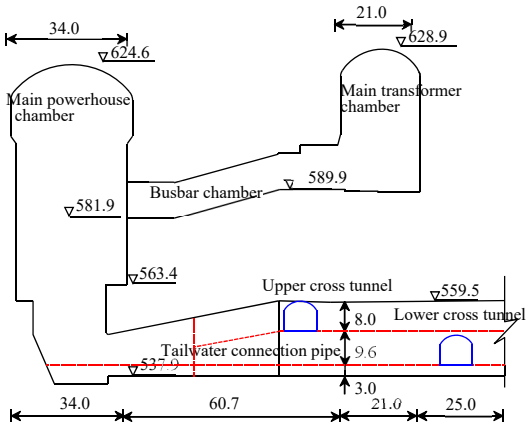

(b) Section of a typical unit in the main cavern of the left bank tailwater connection pipe area (unit: m)

Fig. 1 Layout of main underground chambers at the left bank of Baihetan Hydropower Station

The top arch elevation of the underground powerhouse chamber at the left bank of Baihetan Hydropower Station is 624.6 m, the floor elevation is 535.9 m, the length is 438.0 m, the width below the rock anchor beam is 31.0 m, the above width is 34.0 m, and the axial direction of the chamber is N20ºE. The main transformer chamber is arranged on the downstream side of the main/auxiliary powerhouses, with the length, width and height of 368.0 m, 21.0 m, and 39.5 m, respectively. The net distance between the main transformer chamber and the main/auxiliary powerhouses is 60.7 m. There are 8 tailwater connection pipes located between the main/auxiliary powerhouses and the tailwater surge tank, which are approximately parallel arranged at equal intervals. The axis of the tailwater connection pipe is perpendicular to the axis of the power-house chamber, with a distance of 38.0 m, a cross-section width of 16.0 m, and a height of 20.6. m. It is designed as a 3-layer excavation method (8.0 m for the first layer, 9.6 m for the second layer, and 3.0 m for the third layer) (see Fig.1(b)).

2.2 Engineering geology and in-situ stress conditions of the tailwater connection pipe area

The field survey shows that the $P_2\beta_2^3$ layer of columnar jointed basalt (see Fig.2(a)) is exposed in the tailwater connection pipe area. Its cross-section is mainly a irregular polygon (mainly pentagons and hexagons), with a height of 1−2 m, a side length of 10−25 cm, and an approximately vertical column axis inclination angle of 75º −85º . Inter-column joint surfaces are filled with chlorite film, greasy luster, with hidden joints inside the column. The joints are tightly closed when not excavated, as shown in Fig.2(b).

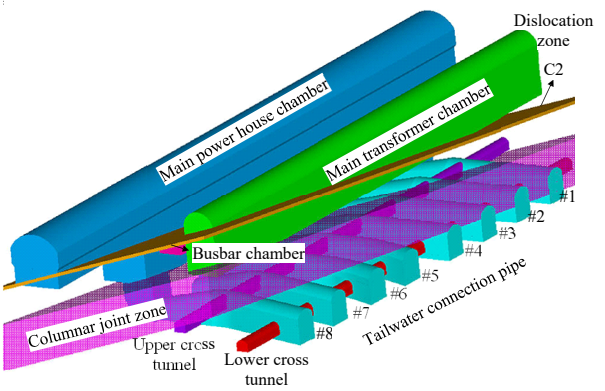

(a) Relationship between columnar joint rock mass and chambers at the tailwater connection pipes

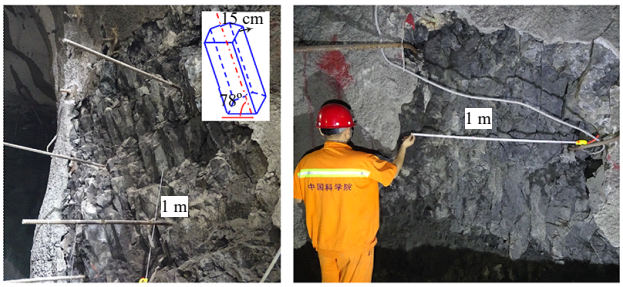

(b) Exposed columnar joint rock mass at the intersection of upper cross tunnel and #7 tailwater connection pipe

Fig. 2 Columnar jointed basalt exposed at the tailwater connection pipe section

The measured in-situ stress and inversion analysis in the chamber area show that the overall in-situ stress in the tailwater connection pipe area is mainly tectonic stress, where the horizontal stress is greater than the vertical stress. The first principal stress is about 21.0−25.0 MPa and its direction is between N30−50º W and

the inclination angle is 5°−13°. The second principal stress value is 15.0−17.0 MPa and the third principal stress value is equivalent to the overlying rock mass, which is between 8.2 and 12.2 MPa[34]. Therefore, the axial direction of the tailwater connection pipe is almost parallel to the direction of maximum principal stress, and the axis of the Upper cross tunnel is almost perpendicular to the maximum principal stress, which is a typical high ground stress environment.

3 Failure characteristics of the columnar jointed rock masses under excavation unloading

3.1 Investigation on the collapse of columnar jointed basalt

When the excavation and blasting of the II layer at section K0+00−K0+16 of the #5 tailwater connection pipe (the intersection with the upper cross tunnel), the second layer of the #8 tailwater connection pipe has been completed, and the #7 and #6 tailwater connection pipes have been constructed beyond the upper cross tunnel, and the #1−#4 tailwater connection pipes are temporarily behind. There are multiple rock mass unloading cracks and local collapse happened at the tailwater connection pipe sidewall and top arch (see Fig.3), where the top arch and spandrel of the upper cross tunnel (between the tailwater connection pipes #4−#8) for the construction of the tailwater connection pipe cracked and collapsed, with the depth of 0.3−0.8 m (locally 1.0−2.0 m) (see Fig.4(a)). A large area of block loss occurred locally at the intersection of the top arch of #7 tailwater connection pipe and upper cross tunnel, with an impact depth of 1.0−2.0 m (locally 3.0−4.0 m) (Fig.4(b)). A collapse occurred at the intersection of the right wall of the #6 tailwater connection pipe and the upper cross tunnel, and the impact depth is 0.3−0.9 m (locally 2.0−4.0 m) (Fig.4(c)). In addition, the #6 tailwater connection pipe and the sidewall of the #5 tailwater connection pipe of the left bank are affected by columnar joints and cracks with steep and gentle angles of inclination, causing a large area of relaxation and collapse failure (Figs.4(d)−4(f)). The specific damage is shown in Table 1 in detail.

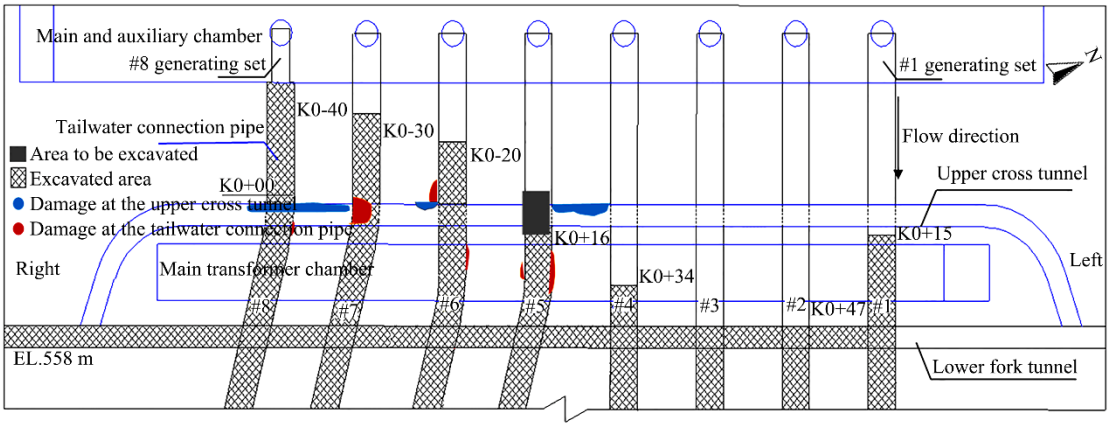

Fig. 3 Distribution of the collapse disaster in columnar jointed rock mass during the construction of tailwater connection pipe

(a) The upstream spandrel of the upper cross tunnel

(b) The top arch of #7 tailwater connection pipe

(c) The right sidewall of #6 tailwater connection pipe

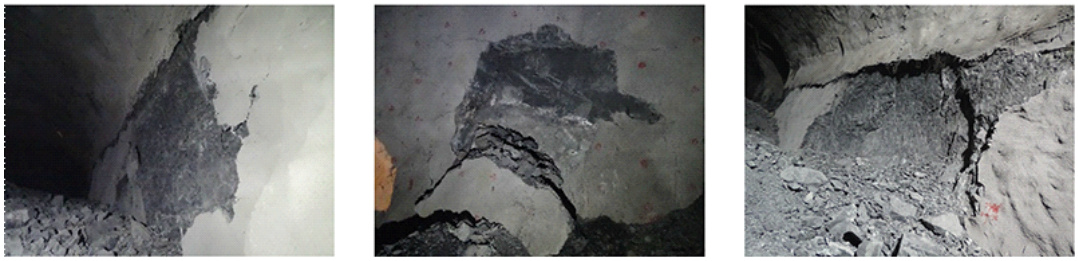

(d) The left sidewall of #6 tailwater connection pipe

(e) The right sidewall of #5 tailwater connection pipe

(f) The left sidewall of #5 tailwater connection pipe

Fig. 4 Typical failure of columnar jointed rock masses around tailwater connection pipes

Table 1 Statistics of the typical failure of the columnar jointed rock masses around the tailwater connection pipe

Damage location	On-site damage	Type of destruction	Destruction size			Special geological conditions
			Length /m	Width /m	Depth /m	
Upper cross tunnel upstream spandrel	Fig.4(a)	Stress collapse	28.0	4.5	0.5−1.0	Cryptocrystalline basalt，Columnar joints
#7 tailwater connection pipe arch（intersect upper cross tunnel）	Fig.4(b)	Stress-structural collapse	14.0	15.0	3.0−4.0	Columnar joints, steeply and gently inclined crack
#6 tailwater connection pipe right side wall（intersect upper cross tunnel）	Fig.4(c)	Stress-structural collapse	9.0	5.0	1.5−2.0	Columnar joints, gently inclined crack
#6 tailwater connection pipe left side wall	Fig.4(d)	Stress-structural collapse	6.0	5.0	0.3	Columnar joints
#5 tailwater connection pipe right side wall	Fig.4(e)	Stress-structural collapse	2.0	3.0	0.5	Columnar joints, gently inclined crack
#5 tailwater connection pipe left side wall	Fig.4(f)	Stress-structural collapse	14.0	10.0	1.0−1.5	Columnar joints, steeply and gently inclined crack

3.2 Collapse characteristics of typical columnar jointed basalts

3.2.1 Stress-structural collapse of #5 tailwater connection pipe

Preliminary investigation shows that the II layer left wall of the #5 tailwater connection pipe has a stress-structural collapse. The columnar jointed rock masses are well developed in this area, with multiple sets of steeply and gently inclined cracks. The jointed cracks are opened after unloading, leading to the poor lithology. It is close to the excavation and blasting area, and the blasting disturbance effect is obvious. In addition, only simple support by wire mesh and shotcrete is carried out after the excavation instead of effective support measures such as bolts and cables to control the rock. Thus the surrounding rock in this area is progressively failed (Fig.5).

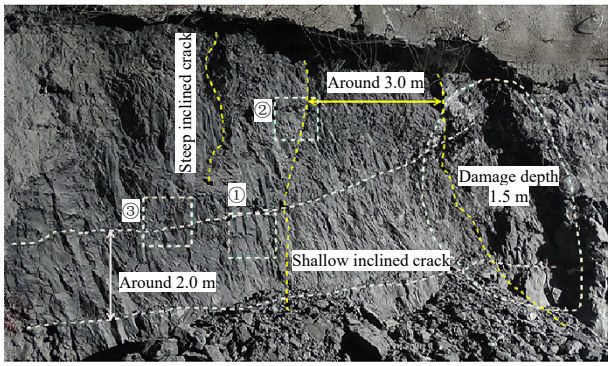

(a) The left wall of II layer of #5 tailwater connection pipe

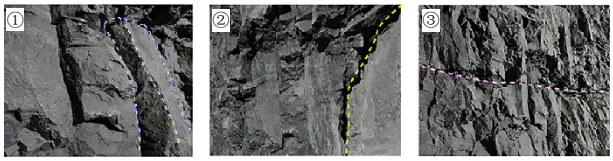

(b) Typical columnar jointed rock mass (c) Steeply inclined crack (d) Gently inclined crack

Fig. 5 Collapse at the left wall of #5 tailwater connection pipe

3.2.2 The stress-structural collapse of #6 tailwater connection pipe

Preliminary investigation showed that the #6 tailwater connection pipe collapsed at the intersection of the tailwater connection pipe right wall and the upper cross tunnel. The columnar jointed rock mass was developed with multiple sets of steeply and gently inclined cracks, and it also suffers a significant blasting disturbance effect as it is close to the excavation face. At the intersections, multiple free surfaces lead to strong unloading, further inducing unloading and relaxation of basalt joints. After the excavation, only simple support with wire mesh and shotcrete is performed, which fails to effectively control the relaxation and cracking of columnar jointed rock mass after stress unloading. The columnar jointed basalt in this area relaxes and fails, and then the entire rock mass disintegrates and collapses (see Fig.6).

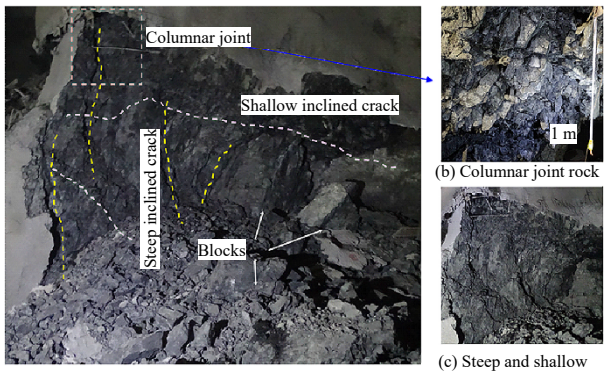

(a) #6 tailwater connection pipe right wall (b) Columnar joint rock (c) Steep and shallow inclined crack

Fig. 6 Collapse at the intersection of the right wall of #6 tailwater connection pipe and the upper cross tunnel

4 In-situ tests of the unloading relaxation of columnar jointed basalt

To gain a deeper understanding of the relaxation depth and internal cracking characteristics of the surrounding rocks in the columnar jointed basalt collapsed area, ultrasonic wave and borehole camera measurements were conducted in the collapsed columnar jointed rock mass area of the tailwater connection pipes. A total of 4 groups (8 test boreholes) were located at the II layer sidewall of the #5, #6 and #7 tailwater connection pipes, with the spacing of 1 m, and the hole depth of 8 m. Each group of test

holes were arranged in a parallel direction, as shown in Figs. 7(a) and 7(b). The test holes 5-1 and 5-2 were located near the damaged right wall of the #5 tailwater connection pipe, and the test holes 5-3 and 5-4 were located near the collapse of the left wall of #5 tailwater connection pipe (see Fig.7(b)).

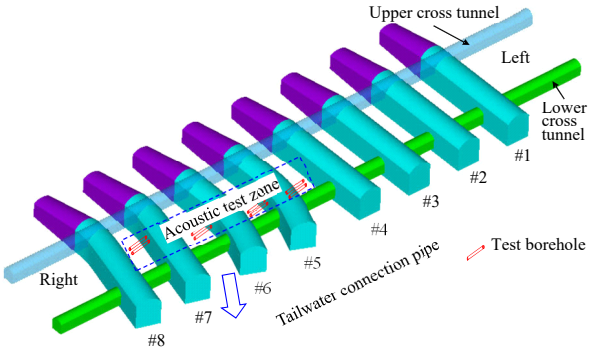

(a) Tailwater connection pipe location

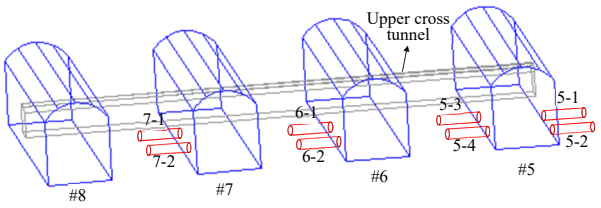

(b) Test borehole distribution

Fig. 7 Distribution of test boreholes at tailwater connection pipe

4.1 Ultrasonic testing of the relaxation characteristics of the columnar joint basalt

Acoustic testing is often used in engineering to reveal the unloading and relaxation characteristics of surrounding rock after cavern excavation. The criterion for determining the depth of rock mass relaxation is based on the obvious inflexion point of the wave velocity curve[24−25]. The results of multiple in-hole ultrasonic tests on the 8 measuring holes of the tailwater connection pipe are (as shown in Fig.8): (i) The wave velocity of the shallow layer in the relaxation zone is generally less than 3.5 km /s, indicating that the surrounding rock in this area is severely relaxed, and micro-cracks or macro-cracks tend to open. (ii) The wave velocity in the unrelaxed area is about 5.5 km /s, indicating that the rock mass in this part is relatively dense and undisturbed. (iii) There is an undisturbed area in the surrounding rock. The local sonic wave velocity drops around 4.2 km /s, indicating that there are numerous micro-cracks or local unloading areas in this area. Overall, the relaxation depth of the tailwater connection pipe is about 1.4 to 3.3 m, and the relaxation depth of each hole is shown in Table 2 in detail. The results of multiple measurements show that the relaxation depth has a slowly increasing trend with time, and the average wave velocity of rock masses has a decreasing trend, indicating that the unloading relaxation degree of columnar jointed rock mass has time-dependent deterioration characteristics and the relaxation depth has a gradual development trend.

4.2 Borehole camera observation of columnar joint basalt cracking

To study the internal joints more intuitively in the excavation damaged zone of the columnar jointed rock mass, borehole cameras were used to observe the internal cracking characteristics of columnar jointed basalt. Observations show that the overall lithology of the columnar jointed rock mass around the tailwater connection pipe is poor. There are many macroscopic joints/cracks within 1 m of the shallow surface layer of the surrounding rock, with a width of 1 to 3 cm and a maximum of 5 cm. The visible open joint plane extends to a depth of 2 m from the orifice, indicating that the shallow surface rock mass has experienced severely unloading relaxation and cracking, and there is a risk of collapse. There are macroscopic cracks in the deep surrounding rock, with a width between 2 and 8 cm. In addition, many micro-cracks are distributed in a tightly closed state, indicating that the lithology of the columnar jointed rock mass is poor. The micro-cracks are in a closed state when there is no excavation disturbance, and the rock mass has no obvious damage, but a great potential risk of unloading and relaxation failure still exists. The typical borehole camera test results are shown in Fig.9.

The comparison and analysis between borehole camera and acoustic test results illustrate that (i) the shallow surface layer of the tailwater connection pipe surrounding columnar joint basalt rock is affected by the excavation and unloading; the joint surfaces between the columns are open, forming macroscopic cracks, and there is a risk of collapse; and (ii) the overall lithology of the surrounding rock of the rock mass is poor, and internal cracks are relatively developed (see Fig.10).

5 Numerical back analysis of the unloading mechanical behavior of the columnar jointed basalt under high stresses

5.1 Numerical back analysis of mechanical response of the excavation of surrounding rocks in the tailwater connection pipe area

5.1.1 Numerical model and parameters

The three-dimensional numerical model is mainly focused on the tailwater connection pipe area. In order to consider the influence of surrounding caverns and unfavorable geological structures, the geometric model of the main caverns includes the following aspects: (a) #1−#8 tailwater connection pipes and the upper and lower cross tunnels at the left bank; (b) The adjacent main powerhouse, main transformer room, and busbar tunnel; and (c) C_2 dislocation zone. For the convenience

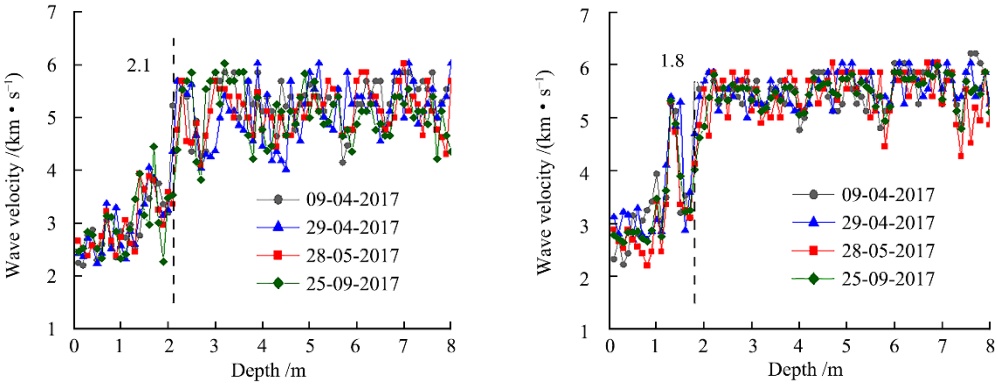

(a) Relaxation depth of borehole 5-1

(b) Relaxation depth of borehole 5-2

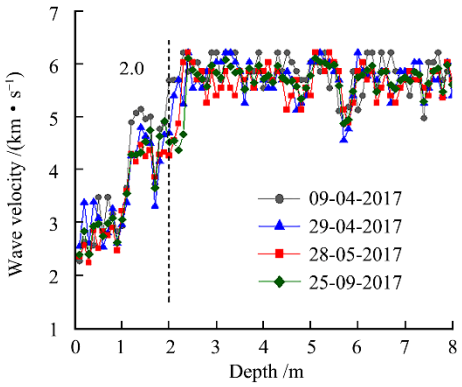

(c) Relaxation depth of borehole 5-3

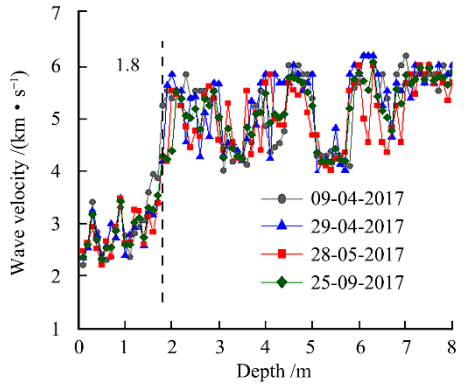

(d) Relaxation depth of borehole 5-4

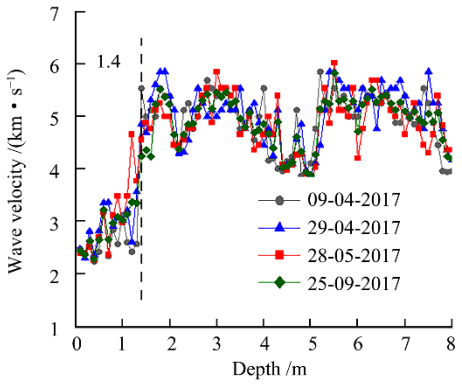

(e) Relaxation depth of borehole 6-1

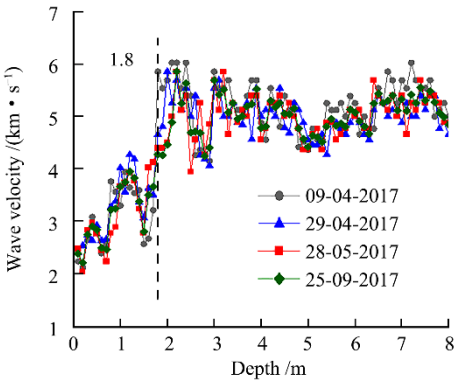

(f) Relaxation depth of borehole 6-2

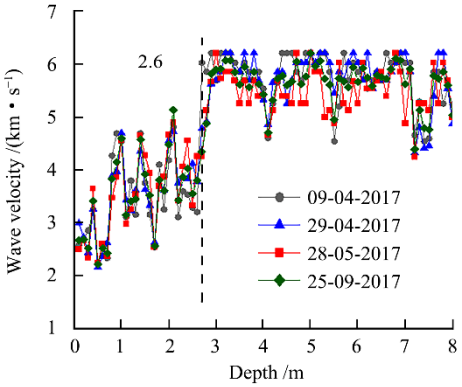

(g) Relaxation depth of borehole 7-1

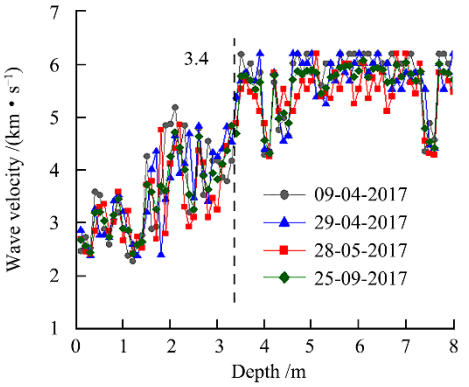

(h) Relaxation depth of borehole 7-2

Fig. 8 Results of relaxation depth at the tailwater connection pipes based on the acoustic test

Table 2 Relaxation depth at the test holes around the tailwater connection pipe

Date	Relaxation depth of each borehole /m							
	5-1	5-2	5-3	5-4	6-1	6-2	7-1	7-2
09-04-2017	2.1	1.8	2.0	1.8	1.4	1.8	2.7	3.4
29-04-2017	2.2	1.9	2.1	1.9	1.6	2.0	2.8	3.4
28-05-2017	2.3	2.0	2.3	2.0	1.7	2.1	2.9	3.5
25-07-2017	2.3	2.1	2.4	2.1	1.7	2.2	2.9	3.5

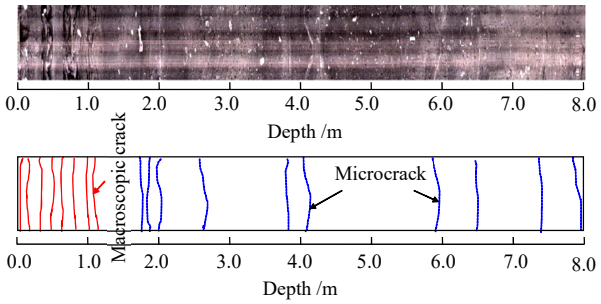

(a) Left wall borehole 5-3 at #5 tailwater connection pipe

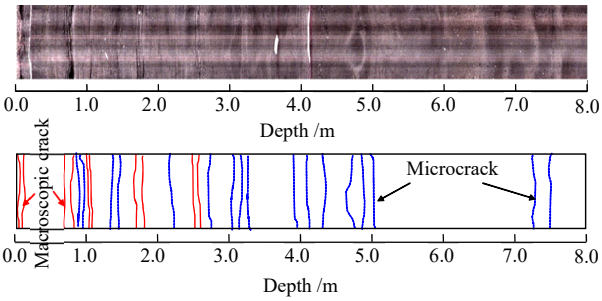

(b) Left wall borehole 7-1at #7 tailwater connection pipe

Fig. 9 Typical results of borehole camera tests at tailwater connection pipe

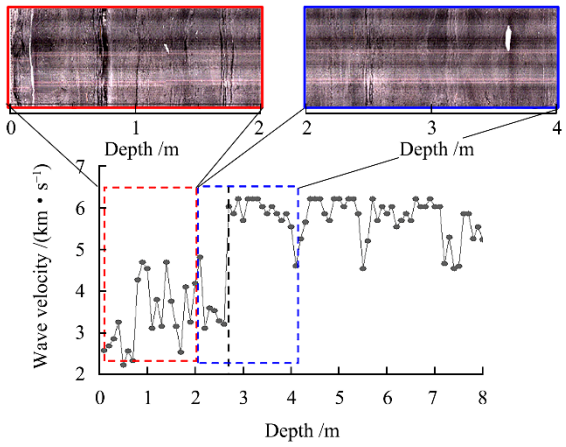

Fig. 10 Comparison between the results of acoustic test and borehole test (hole 7-1)

of analysis, two sections are cut for visual display, namely the section A along the axis of the upper cross tunnel and the section B at a height of 1 m from the excavation surface of the II layer, as shown in Fig.11.

The columnar jointed rock mass contains inter-column joint planes with 'polygonal grid characteristics' in the cross-section, and a large number of hidden joint planes exist inside the column. Numerous field tests[21−23] show that the columnar jointed rock mass exhibits transverse isotropy characteristics. Based on the unique joint network structure characteristics, the transversely isotropic deformation characteristics and the strength characteristics of columnar joints, a columnar joint rock mass mechanical model incorporating multiple sets of joint strength criteria[35] is adopted. Secondary development using VC++ language is embedded into commercial software to perform numerical calculation and analysis. The calculation formula for the stiffness matrix of the transversely isotropic deformation is

$$[K]=\begin{bmatrix} C_{11} & C_{12} & C_{13} & 0 & 0 & 0 \\ C_{12} & C_{22} & C_{13} & 0 & 0 & 0 \\ C_{13} & C_{13} & C_{33} & 0 & 0 & 0 \\ 0 & 0 & 0 & C_{44} & 0 & 0 \\ 0 & 0 & 0 & 0 & C_{66} & 0 \\ 0 & 0 & 0 & 0 & 0 & C_{66} \end{bmatrix} \tag{1}$$

$$\left.\begin{aligned} C_{11}=C_{22}&=\frac{E_1(1-n\mu_{13}^2)}{(1+\mu_{12})(1-\mu_{12}-2n\mu_{13}^2)} \\ C_{12}&=\frac{E_1(\mu_{12}+n\mu_{13}^2)}{(1+\mu_{12})(1-\mu_{12}-2n\mu_{13}^2)} \\ C_{13}&=\frac{E_1\mu_{13}}{1-\mu_{12}-2n\mu_{13}^2},\ C_{33}=\frac{E_3(1-\mu_{12})}{1-\mu_{12}-2n\mu_{13}^2} \\ C_{44}&=\frac{E_1}{1+\mu_{12}},\ C_{66}=2G_{13},\ n=\frac{E_1}{E_3} \end{aligned}\right\} \tag{2}$$

where E_1 and μ_{12} are the elastic modulus and Poisson's ratio perpendicular to the axial direction of the cylinder; E_3, μ_{13} and G_{13} are the elastic modulus, Poisson's ratio and shear modulus parallel to the axial direction of the cylinder, respectively.

Regarding the shear and tensile failure of the intact rock mass and joints the unloaded columnar jointed basalt, a combined strength criterion is adopted:

(1) For the failure of an intact rock block, the Mohr-Coulomb strength criterion with a tensile cut-off is used.

(2) For the rough surface of the inter-column joint, the Barton-Bandis strength criterion with a tensile cut-off is used:

$$\left.\begin{aligned} f_i^{\mathrm{s}}&=\tau_i-\sigma_{3'3'}^i\tan\varphi_{\mathrm{m}}^i \\ \varphi_{\mathrm{m}}^i&=\mathrm{JRC}^i\lg\left(\frac{\mathrm{JCS}^i}{|\sigma_{3'3'}^i|}\right)+\varphi_{\mathrm{j}}^i \\ f_i^{\mathrm{t}}&=\sigma_{3'3'}^i-\sigma_{ji}^{\mathrm{t}} \end{aligned}\right\} \tag{3}$$

where φ_{m}^i, φ_{j}^i, JRC^i and JCS^i are the friction angle, residual friction angle, joint roughness coefficient and joint wall strength of the i-th set of joint surfaces, respectively; τ_i, $\sigma_{3'3'}^i$ and σ_{ji}^{t} are the shear stress, normal stress and tensile strength of the i-th set of joint surfaces strength, respectively.

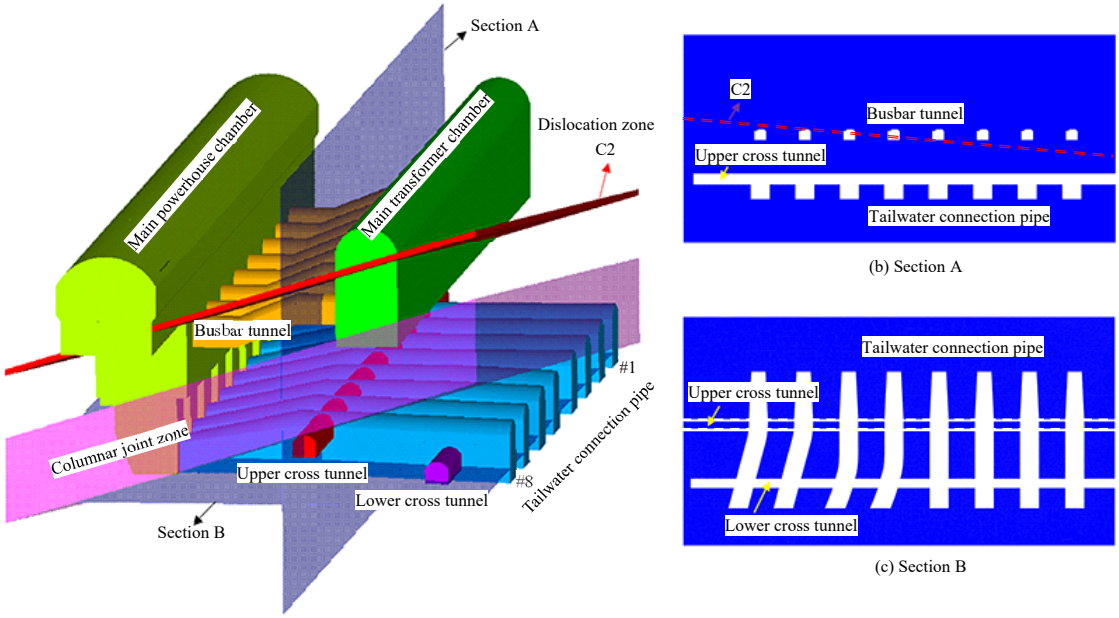

(a) Geometric model

(b) Section A

(c) Section B

Fig. 11 Geometric model of caverns in the left bank of tailwater connection pipe of Baihetan Hydropower station and its section

(3) For the hidden joint surface inside the cylinder, the Mohr-Coulomb strength criterion with a tensile cut-off is used:

$$f_{j3}^{\mathrm{s}} = \tau_{j3} - \sigma_{3'3'} \tan\varphi_{j3} - c_{j3} \tag{4}$$

$$f_{j3}^{\mathrm{t}} = \sigma_{3'3'} - \sigma_{j3}^{\mathrm{t}} \tag{5}$$

$$h_{j3} = \tau_{j3} + \sigma_{j3}^{\mathrm{t}} \tan\varphi_{j3} - c_{j3} + \left(\sqrt{1+\tan^2\varphi_{j3}} - \tan\varphi_{j3}\right) \tag{6}$$

where f_{j3}^{s}, f_{j3}^{t} and h_{j3} are the functions of the shear yield criterion, tensile yield criterion, and shear−tension mixed yield criterion of the hidden joint surface; τ_{j3} and $\sigma_{3'3'}$ are the shear and normal stress acting on the hidden joint surface; c_{j3}, φ_{j3} and σ_{j3}^{t} are the cohesion, internal friction angle and tensile strength of the hidden joint surface; c_0, φ_0 and σ^t are the cohesion, internal friction angle and tensile strength of the rock block, respectively. The mechanical parameters are determined based on the inversion of the diversion tunnel[36−37], see Tables 3 and 4 for details.

Table 3 Mechanical parameters of rock masses in the columnar jointed basalt

Parameters	E_1 /GPa	E_3 /GPa	μ_{12}	μ_{13}	G_{13} /GPa	c_0 /MPa	φ_0 /(°)	σ^t /MPa
Value	10.5	8.6	0.26	0.26	8.43	3	36	1.2

Table 4 Mechanical parameters of joints in the columnar jointed basalt

Parameters	JRC^i /GPa	JCS^i /GPa	φ_j^i /(°)	σ_{ji}^t /MPa	c_{j3} /MPa	φ_{j3} /(°)	σ_{j3}^{t} /MPa
Value	13	115	32	0.22	0.35	20	0.05

5.1.2 Mechanical response of the surrounding rock under excavation unloading

The deformation distribution law and the maximum principal stress concentration of surrounding rocks after excavation and unloading can reflect, to a certain extent, the possible location and potential risk of surrounding rock failure after cavern excavation. Meanwhile, rock fracture degree (RFD) is used as the evaluation index of surrounding rock fracture[38], which can quantitatively characterize the fracture degree of surrounding rock. Generally, an area with RFD $\geqslant$ 1.0 is defined as the fracture depth range and RFD = 2.0 means that the surrounding rock is completely fractured. Thus the unification of numerically calculated relaxation and fracture zone with the on-site measured relaxation depth and the visible fracture depth of surrounding rock is achieved. Therefore, this article will analyze the stability of surrounding rock of tailwater connection pipe under the current excavation state from three aspects of surrounding rock deformation, stress and fracture index RFD, as follows:

(1) With the excavation of the tailwater connection pipe II layer, the overall deformation of top arch and left spandrel is large, generally greater than 30 mm, and the deformation of sidewall is between 15 and 25 mm (Fig.12). The arch of the upper cross tunnel and its downstream spandrel have a large deformation, locally reaching 35 mm. The displacement value shows a trend of increasing gradually from #8 to #1 tailwater connection pipes, which is related to the inclined dislocation zone towards #1 tailwater connection pipe. At the intersection of the tailwater connection pipe and upper cross tunnel, the displacement value exceeds 35 mm, forming a large

risk of local stability, which should be paid more attention to.

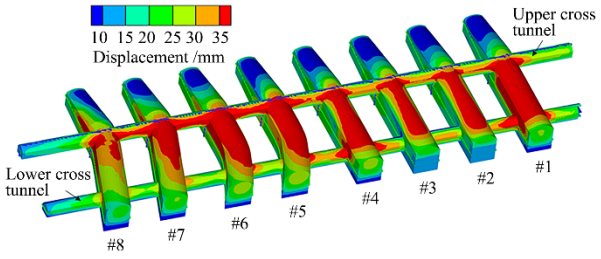

(a) Tailwater connection pipe

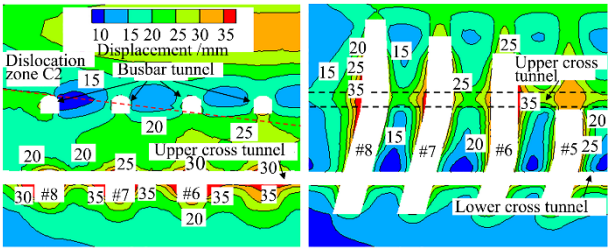

(b) Displacement at section A (c) Displacement at section B

Fig. 12 Characteristics of rock masses displacement distributions during the II layer excavation(unit: mm)

(2) The stresses at the tailwater connection pipe and the surrounding rock of the upper cross tunnel are adjusted and deflected during excavation of the tailwater connection pipe II layer, and stress concentration occurs at the top arch position, with a locally maximum principal stress of 40 MPa (Fig.13). The stress concentration effect of surrounding rock at the intersection of the tailwater connection pipe and upper cross tunnel is obvious. The minimum principal stresses of surrounding rock surface at the sidewall of tailwater connection pipe and the intersection with upper cross tunnel are all less than 5 MPa (Fig.14), indicating the surrounding rock has an obvious unloading effect after excavation, where the joint surface of the surrounding columnar jointed rock mass prone to open failure in the state of excavation and unloading.

(3) The tailwater connection pipe and top arch of the upper cross tunnel have unloading relaxation areas during excavation of the tailwater connection pipe II

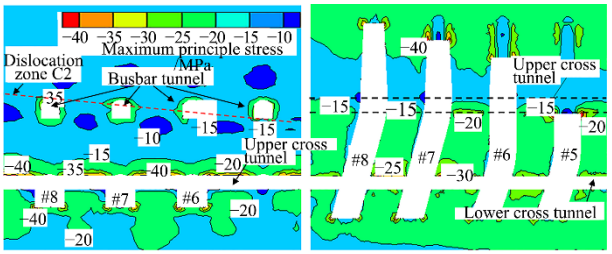

(a) Maximum principle stress at section A (b) Maximum principle stress at section B

Fig. 13 Characteristics of maximum rock masses principal stress distributions during the II layer excavation(unit: MPa)

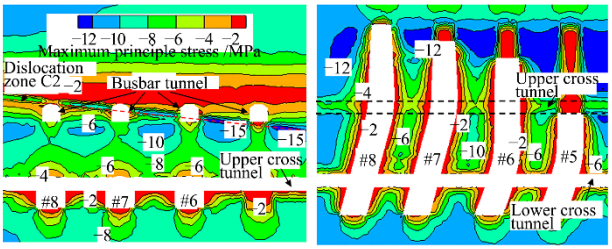

(a) Minimum principle stress at section A (b) Minimum principle stress at section B

Fig. 14 Characteristics of minimum rock masses principal stress distributions during the II layer excavation at left tailwater connection pipe (unit: MPa)

layer (Fig.15), with an average of 1 to 2 m (locally 2 to 3 m) which is consistent with the location of the fork tunnel collapse failure. The sidewall has a certain unloading relaxation phenomenon, with an average of 1 to 2 m, which is consistent with the damage, acoustic and borehole camera results of the left and right side walls of the #5 and #6 tailwater connection pipes. The unloading area of tunnel excavation is large at the intersection of the tailwater connection pipe and the upper cross tunnel, generally 2 to 4 m, and the depth and relaxation damage are also increased sharply, which is consistent with the large stress-structural collapse at the intersection of the #6 tailwater connection pipe and upper cross tunnel.

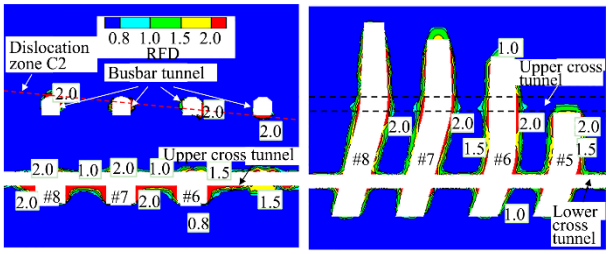

(a) RFD at section A (b) RFD at section B

Fig. 15 Characteristics of rock masses RFD distributions during the II layer excavation at left tailwater connection pipe

5.2 Stress-structural collapse mechanism

Based on the field investigation, in-situ test and numerical back analysis of the columnar jointed rock mass destruction, the stress-structural collapse of the columnar jointed rock mass can be summarized as follows: under the stress state adjustment of cavern excavation, the columnar jointed rock mass is unloaded and relaxed. This causes the columnar rock mass structural plane to undergo expansion and structural deterioration. The rock mass structure deteriorates and is affected by the cutting of the near-horizontal joint plane, which leads to the fracture of the rock column and further cause continuous unloading and relaxation to the large-scale collapse of chain catastrophic damage. Essentially, the deterioration and catastrophe of columnar jointed rock mass are driven by the change in the stress state of the columnar jointed surrounding rock, that is,

the excavation of multiple caverns leads to strong unloading of the rock mass. After the stress redistribution, the second and third principal stresses decrease while the first principal stress increases in the intersection area of the surrounding rock. The strong unloading effect produced by the decrease of confining pressure causes the joint planes of the columnar jointed rock mass to relax and crack, while the increase of the maximum principal stress causes the column to break, resulting in a collapse (see Fig.16). Overall, the stress-structural collapse of the columnar jointed rock mass of the Baihetan tailwater connection pipe contains two failure modes:

(1) Sidewall slip→slide mode. For the sidewall area columnar jointed surrounding rock, the surface surrounding rock of sidewall is in a state of unloading and rebounding after the cavern excavation. The joint surfaces between the original closed columns relax and expand, and the blasting damage effect causes the joint surfaces between columns to open. A permeable sliding surface along the inter-column joint and hidden joint surface in the column forms, causing the column to slip and collapse (see Fig.16(a)).

(2) Top arch fracture→fall mode. After the excavation of the cavern, the arch is in a state of stress concentration. The columnar basalt rock block of the arch is broken or split along the hidden joint plane of the columnar jointed rock mass. Shallow fractured basalt and primary columnar joint planes cut each other and form fragmented blocks. The blocks fall under their own weight, and the fracturing gradually develops inward, resulting in a certain volume of collapse (see Fig.16(b)).

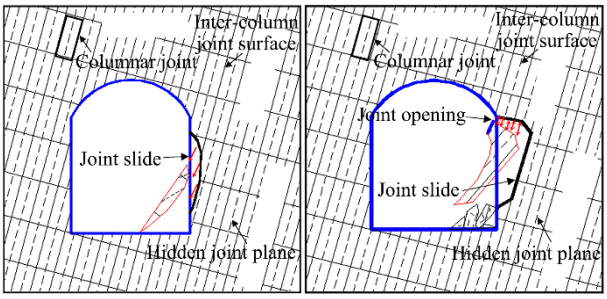

(a) Slip−slide failure mode of the sidewall columnar joint rock mass

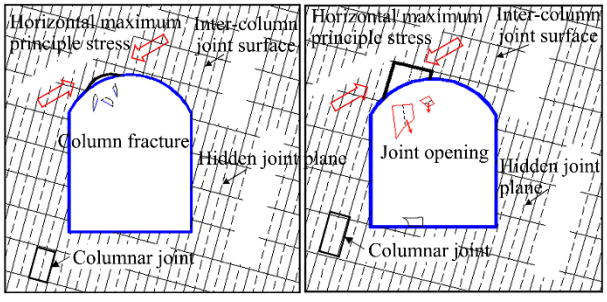

(b) Fracture−fall failure mode of the top arch columnar joint rock mass

Fig. 16 Schematic of the collapse mechanism in columnar jointed rock mass

5.3 Support measures

The excavation of underground caverns under high stress has a more significant excavation unloading effect, especially in the intersecting area of multiple caverns. Columnar jointed rock mass contains many inter-column joint planes and hidden joint planes in the columns, the rock mass breaks abnormally, and the joint planes will be coalesced to form small blocks under the action of excavation and unloading, causing the column to fracture and collapse or slip−slide. Therefore, a reasonable excavation plan should be adopted to reduce the unloading effect, and necessary support measures should be taken to restrain the degeneration of mechanical properties of column jointed rock masses[38]. In general, for the excavation and support of surrounding rock in the columnar joint area of the tailwater connection pipe, the following points should be considered such as short advancement, weak blasting, layered excavation. They are used to improve the stress state of the surrounding rock. After construction of the upper cross tunnel is completed, its plugging should be completed as soon as possible to reduce the stress release of the surrounding rock.

After the excavation, high-strength protective layer materials such as nano-steel fibre concrete are sprayed in time, such as primary spray steel fiber concrete of 5 cm, wire mesh Φ8 mm@15 cm×15 cm, and re-spray concrete 10 cm to maintain the columnar jointed rock mass cohesion as much as possible. At the same time, the systematic prestressed bolt support is carried out in time to improve the tensile and shear resistance of the columnar jointed rock mass, and the corresponding support parameters are as Φ32 mm, length L = 9 m, prestress T = 100 kN, spacing 2 m×2 m, as shown in Fig.17(a).

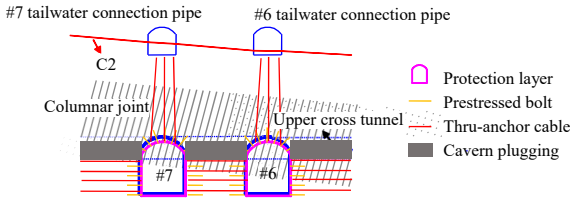

(a) Scheme diagram of the support

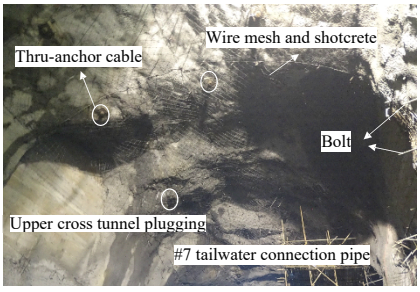

(b) Support result

Fig. 17 Reinforced supporting scheme for columnar jointed basalt at tailwater connection pipe

For the columnar jointed rock mass in the damaged area, in addition to the above supporting measures, the counter-crossing pre-stressed anchor cable through the tailwater connection pipe is carried out at the damaged position. The anchor cable supporting parameter are: T = 2 500 kN, and the spacing is 3.6−6.0 m. For example, at the damage positions of the #7 tailwater connection pipe and the top arch of the upper cross tunnel, pre-stressed anchor cable supports are conducted at the corresponding position of the tailwater connection pipe and the bus tunnel. The adjacent damage area at the tailwater connection pipes of #5, #6 tailwater connection pipe sidewall should also carry out the anchor cable support (Fig.17(b)).

6 Conclusions

Based on the investigation and study of columnar jointed rock mass stress-structural collapse on the left bank of Baihetan Hydropower Station, this paper analyzed the stress-structural collapse failure mechanism and proposed corresponding control measures by the approaches of ultrasonic wave and borehole camera measurements, combined with numerical calculation methods. The main understandings and conclusions include:

(1) On-site investigation and comprehensive tests show that the internal joints of columnar joint basalt of the tailwater connection pipe are dense, and the behaviors of relaxation and joint surface opening are shown after excavation and unloading. Continuous field observation results reveal that the unloading relaxation depth of columnar jointed rock masses is slowly increasing, that is, the unloading relaxation failure is time-dependent.

(2) Numerical calculations show that the large-area excavation of the tailwater connection pipe and its upper cross tunnel leads to the surrounding rock being in a two-way or one-way stress state, where the stress unloading effect is obvious and the confining pressure of surrounding rock is significantly reduced. In addition, the excavation disturbance of adjacent caverns also directly promotes the unloading relaxation and cracking of columnar jointed basalt.

(3) The inherent cause of the collapse failure of the tailwater connection pipe and its upper cross tunnel in high-stress areas can be considered as the redistribution of surrounding rock stress after the cavern excavation. The strong unloading and relaxation of the columnar jointed basalt cause the opening of its internal joint surface and structural deterioration, which in turn leads to the fracture and disintegration of the basalt column, and induces a chain catastrophe process of continuous unloading and relaxation of the rock mass→gradual collapse.

(4) According to the analysis of the stress-structural collapse mechanism of the columnar jointed rock mass, technical measures such as short advancement, layered and stepped excavation, and weak blasting have been adopted to better control the unloading effect of surrounding columnar jointed rock mass. The high-strength protective layer such as nano steel fibre concrete effectively prevents the shallow layer of columnar jointed rock from tension cracking and its toppling and breaking. The use of pre-stressed bolts and thru-anchor cables directly inhibits the opening and slipping of columnar joints internal joint surface, which further prevents the continuous time-dependent unloading and relaxation of the columnar jointed rock mass.

References

[1] GU De-zhen. Fundamentals of rock mass engineering geomechanics[M]. Beijing: Science Press, 1979.

[2] SUN Guang-zhong. Rock mass structure mechanics[M]. Beijing: Science Press, 1988.

[3] WANG Si-jing. Geological nature of rock and its deduction for rock mechanics[J]. Chinese Journal of Rock Mechanics and Engineering, 2009, 28(3): 433−450.

[4] WEI Zhi-yun, XU Guang-li, SHEN Yan-jun, et al. Characteristics and stability evaluations of diabase dikes group surrounding underground caverns of dagangshan hydropower station[J]. Journal of Engineering Geology, 2013, 21(2): 206−215.

[5] LIU G F, JIANG Q, FENG G L, et al. Microsei- smicity-based method for the dynamic estimation of the potential rockburst scale during tunnel excavation[J]. Bulletin of Engineering Geology and the Environment, 2021, 80(5): 3605−3628.

[6] ZHANG Di, LI Shao-jun, XU Ding-ping, et al. Investigation on deformation and cracking behaviors and stability analysis of surrounding rock mass during the preliminary excavation of underground main powerhouse of Shuangjiangkou hydropower station[J]. Chinese Journal of Rock Mechanics and Engineering, 2021, 40(3): 520−532.

[7] MARTIN C D, KAISER P K, MCCREATH D R. Hoek-Brown parameters for predicting the depth of brittle failure around tunnels[J]. Canadian Geotechnical Journal, 1999, 36(1): 136−151.

[8] XIANG Tian-bing, FENG Xia-ting, JIANG Quan, et al. Failure mode dynamic recognition and control for surrounding rock of large-scale cavern group[J]. Chinese Journal of Rock Mechanics and Engineering, 2011, 30(5): 871−883.

[9] DONG Jia-xing, XU Guang-li, LI Zhi-peng, et al. Classification of failure modes and controlling measures for surrounding rock of large-scale caverns with high geostress[J]. Chinese Journal of Rock Mechanics and Engineering, 2014, 33(11): 2161−2170.

[10] TANG Hui-ming, ZHANG Yi-hu, SUN Yun-zhi. A study of equivalent deformability parameters in rock masses[J]. Earth Science, 2007, 32(3): 389−396.

[11] QIN Juan, GENG Ke-qin. Representative element aggregation model for jointed rock mass and prediction of elastic parameters[J]. Journal of Hydraulic Engineering, 2001, 32(9): 45−50.

[12] ZHANG Zhi-gang, QIAO Chun-sheng. Improved empirical determination of strength parameter for jointed rock masses and its application in engineering[J]. Journal of Beijing Jiaotong University, 2006, 30(4): 46−49.

[13] ZHANG Gui-ke, XU Wei-ya. Analysis of joint network simulation method and REV scale[J]. Rock and Soil Mechanics, 2008, 29(6): 1675−1680.

[14] SINGH M, RAO K S, RAMAMURTHY T. Strength and deformational behaviour of a jointed rock mass[J]. Rock Mechanics and Rock Engineering, 2002, 35(1): 45−64.

[15] IVARS D M, PIERCE M E, DARCEL C, et al. The synthetic rock mass approach for jointed rock mass modelling[J]. International Journal of Rock Mechanics and Mining Sciences, 2011, 48(2): 219−244.

[16] LI Jian-lin, WANG Le-hua. Study on unloading nonlinear mechanical characteristics of jointed rock mass[J]. Chinese Journal of Rock Mechanics and Engineering, 2007, 26(10): 1968−1975.

[17] SHEN Jun-hui, WANG Lan-sheng, WANG Qing-hai, et al. Deformatin and fracture features of unloaded rock mass[J]. Chinese Journal of Rock Mechanics and Engineering, 2003, 22(12): 2028−2031.

[18] XU Wei-ya, ZHENG Wen-tang, SHI An-chi. Classification and quality assessment of irregular columnar jointed basaltic rock mass for hydraulic engineering[J]. Journal of Hydraulic Engineering, 2011, 42(3): 262−270.

[19] FAN Q X, FENG X T, WENG W L, et al. Unloading performances and stabilizing practices for columnar jointed basalt: a case study of Baihetan hydropower station[J]. Journal of Rock Mechanics and Geotechnical Engineering, 2017, 9(6): 1041−1953.

[20] FAN Q X, WANG Z L, XU J R, et al. Study on Deformation and control measures of columnar jointed basalt for Baihetan super-high arch dam foundation[J]. Rock Mechanics and Rock Engineering, 2018, 51(8): 2569−2595.

[21] SHI An-chi, TANG Ming-fa, ZHOU Qi-jian. Research of deformation characteristics of columnar jointed basalt at Baihetan hydropower station on Jinsha river[J]. Chinese Journal of Rock Mechanics and Engineering, 2008, 27(10): 2079−2786.

[22] JIANG Quan, FENG Xia-ting, FAN Yi-lin, et al. Survey and laboratory study of anisotropic properties for columnar jointed basaltic rock mass[J]. Chinese Journal of Rock Mechanics and Engineering, 2013, 32(12): 2527−2535.

[23] JIANG Q, FENG X T, HATZOR Y H, et al. Mechanical anisotropy of columnar jointed basalts: an example from the Baihetan hydropower station, China[J]. Engineering Geology, 2014, 175(3): 35−45.

[24] DUAN S Q, JIANG Q, LIU G F, et al. An insight into the excavation-induced stress paths on mechanical response of weak interlayer zone in underground cavern under high geostress[J]. Rock Mechanics and Rock Engineering, 2021, 54(3): 1331−1354.

[25] PEI Shu-feng, FENG Xia-ting, ZHANG Jian-cong, et al. Time-dependent relaxation characteristics of columnar jointed basalts in high-slope dam foundation during excavation[J]. Rock and Soil Mechanics, 2018, 39(10): 3743−3754.

[26] XIAO Wei-min, DENG Rong-gui, FU Xiao-min, et al. Model experiments on deformation and strength anisotropy of columnar jointed rock masses under uniaxial compression[J]. Chinese Journal of Rock Mechanics and Engineering, 2014, 33(5): 957−963.

[27] XIAO Wei-min, DENG Rong-gui, ZOU Zu-yin. Anisotropic strength criterion for columnar jointed rock masses[J]. Chinese Journal of Rock Mechanics and Engineering, 2015, 34(11): 2205−2214.

[28] JI H, ZHANG J C, XU W Y, et al. Experimental investigation of the anisotropic mechanical properties of a columnar jointed rock mass: observations from laboratory-based physical modelling[J]. Rock Mechanics and Rock Engineering, 2017, 50(7): 1919−1931.

[29] NING Yu, XU Wei-ya, ZHENG Wen-tang, et al. Study of random simulation of columnar jointed rock mass and its representative elementary volume scale[J]. Chinese Journal of Rock Mechanics and Engineering, 2008, 27(6): 1202−1208.

[30] ZHENG Wen-tang, XU Wei-ya, NING Yu, et al. Scale effect and anisotropy of deformation modulus of closely jointed basaltic mass[J]. Journal of Engineering Geology, 2010, 18(4): 559−565.

[31] DI S J, XU W Y, NING Y, et al. Macro-mechanical properties of columnar jointed basaltic rock masses[J]. Journal of Central South University of Technology, 2011, 18(6): 2143−2149.

[32] ZHONG Shi-ying, XU Wei-ya. Anisotropic failure criterion incorporating microstructure tensor for rock mass with columnar joints[J]. Rock and Soil Mechanics, 2011, 32(10): 3081−3084.

[33] YAN Dong-xu, XU Wei-ya, WANG Wei, et al. Research of size effect on equivalent elastic modulus of columnar jointed rock mass[J]. Chinese Journal of Geotechnical Engineering, 2012, 34(2): 243−250.

[34] Huadong Engineering Corporation Limited of Hydro China Corporation. Special report on stability of surrounding rock of underground powerhouse caves of Baihetan hydropower station, Jinsha River (The excavation of floor VIII on the left bank was completed)[R]. Hangzhou: Hydro China Huadong Engineering Corporation, 2017.

[35] HAO X J, FENG X T, YANG C X, et al. Analysis of EDZ development of columnar jointed rock mass in the Baihetan diversion tunnel[J]. Rock Mechanics and Rock Engineering, 2016, 49(4): 1289−1312.

[36] HAO Xian-jie, FENG Xia-ting, JIANG Quan, et al. Research on unloading failure mechanism of columnar Jointed rock mass in tunnel based on scanning electron microscopy experiments[J]. Chinese Journal of Rock Mechanics and Engineering, 2013, 32(8): 1647−1655.

[37] HAO Xian-jie. Time-dependent excavation damaged zone development of columnar jointed rock mass and cracking restraint method for hard rock tunnels[D]. Wuhan: Institute of Rock and Soil Mechanics, Chinese Academy of Sciences, 2015.

[38] JIANG Quan, FENG Xia-ting, LI Shao-jun, et al. Cracking-restraint design method for large underground caverns with hard rock under high geostress condition and its practical application[J]. Chinese Journal of Rock Mechanics and Engineering, 2019, 38(6): 1081−1101.